


Cite this: *J. Mater. Chem. C*, 2020, **8**, 11929

Molecular doping in few-molecule polymer-dopant complexes shows reduced Coulomb binding

Chuan-ding Dong ^{*a} and Stefan Schumacher^{ab}

The mechanistic study of molecular doping of organic semiconductors (OSC) requires an improved understanding of the role and formation of integer charge transfer complexes (ICTC) on a microscopic level. In the present work we go one crucial step beyond the simplest scenario of an isolated bi-molecular ICTC and study ICTCs formed of up to two poly[2,6-(4,4-bis(2-ethylhexyl)-4*H*-cyclopenta[2,1-*b*,3,4-*b'*])dithiophene)-*alt*-4,7-(2,1,3-benzothiadiazole)] (PCPDT-BT) oligomers and up to two CN6-CP molecules. We find that depending on geometric arrangement, complexes containing two conjugated oligomers and two dopant molecules can show p-type doping with double integer charge transfer, resulting in either two singly doped oligomers or one doubly doped oligomer. Interestingly, compared to an individual oligomer-dopant complex, the resulting in-gap states on the doped oligomers are significantly lowered in energy. Indicating that, already in the relatively small systems studied here, Coulomb binding of the doping-induced positive charge to the counter-ion is reduced which is an elemental step towards generating mobile charge carriers through molecular doping.

Received 4th May 2020,
Accepted 31st July 2020

DOI: 10.1039/d0tc02185g

rsc.li/materials-c

1 Introduction

Molecular doping plays a crucial role in the functionalization of organic semiconductors (OSC).^{1–4} However, the underlying microscopic mechanisms are not yet fully understood in spite of increasing research efforts into charge transfer (CT) processes in doped molecular films.^{5–9} The primary CT in p-type doping is achieved when one electron migrates from a semi-conducting polymer chain onto a dopant molecule, resulting in the formation of an ion pair, a so-called integer charge transfer complex (ICTC). While the electronic hybridization between OSC chains and dopant molecules is also an important process for many systems,^{10–12} formation of ICTCs is considered crucial for efficient charge carrier generation¹³ and is evidenced in doped conjugated molecular films using UV-Vis optical^{7,11–19} or vibrational spectroscopy.^{20,21} However, the charge generation process involving ICTCs, where the hole is released to form a mobile charge carrier in the OSC matrix, from a microscopic perspective of individual ICTCs remains elusive. This is mainly because of the expected strong Coulomb attraction of the hole to the corresponding negatively charged counter ion in the OSC

environment of low electrical permittivity, which contradicts the rather high doping efficiency and resulting electric conductivity typically observed in doped molecular films. For the latter, the energetic disorder in the doped OSC matrix and the change of energetic landscape caused by the formation of ICTCs are thought to play an important role,^{22,23} and the associated factors such as Fermi level shifting with doping concentration were also discussed.¹² In particular, the mechanism that the overlapping Coulomb potentials from the neighbouring dopant molecules in the matrix smear each other out and lead to enhanced charge transportation was proposed.^{22,24} Recent reports also demonstrate the possibility to minimize the Coulomb binding energy by modifying the chemical structure of the dopant, resulting in enhanced thermal activation of the charge carries already at low doping concentration.²³

In many aspects, the detailed theoretical understanding of the underlying molecular doping mechanisms in macroscopic OSC films is still lagging behind the experimental progress in this area.⁶ In order to reduce this gap and to obtain additional valuable insights on a microscopic level that is typically experimentally not directly accessible, density functional theory (DFT) approaches are often applied as the method of choice to study the molecular building blocks of doped OSC films. This has been done for a large number of different materials to address conformational and electronic properties, including the frontier electronic energy levels, density of states (DOS), and their variation with size and conjugation length. Also bi-molecular

^a Department of Physics and Center for Optoelectronics and Photonics Paderborn (CeOPP), Paderborn University, Warburger Strasse 100, 33098 Paderborn, Germany. E-mail: cddong@mail.uni-paderborn.de

^b James C. Wyant College of Optical Sciences, University of Arizona, Tucson, AZ 85721, USA

OSC:dopant complexes were studied,^{25–27} including studies on their vibrational properties and optical excitations in direct comparison with experiments.^{20,28–31} However, studies using quantum-chemical methods explicitly reporting on ICTC formation are only scarce. This is mainly because an *ab initio* theoretical description of integer charge transfer in the system's electronic ground state in principle calls for a multi-determinant treatment, which is computationally extremely challenging even for systems of small sizes. As a remedy, in our recent work on the PCPDT-BT co-polymer combined with a series of commonly used molecular dopants we have reported that physically meaningful results can be obtained using broken-symmetry (BS) DFT calculations. These represent an approximate treatment but are able to explicitly capture both partial charge transfer through orbital hybridization and integer charge transfer within the same unified theoretical approach at moderate computational cost.^{20,25}

In order to obtain a more in-depth and microscopic understanding of the role ICTCs play in the p-type doping of OSCs, it is essential to explicitly include part of the electronic environment provided by the molecules surrounding a given ICTC.^{32–34} In the present work as a representative example we study PCPDT-BT:CN6-CP complexes containing up to two PCPDT-BT oligomers and two CN6-CP dopants arranged in different geometrical settings. Based on our BS DFT calculations we find that complexes consisting of two PCPDT-BT oligomers and two CN6-CP molecules, depending on their geometrical arrangement can show two different types of ICT, either resulting in one doubly-doped oligomer or two singly doped ones. Our calculations also demonstrate that compared to individual ICT complexes, these larger complexes possess a reduced energy cost for releasing a hole as a free charge carrier.

2 Computational details

Following our previous work,²⁵ in the present work we use broken-symmetry (BS) density functional theory (DFT) calculations to study the electronic states of different molecular complexes. By allowing different spatial orbitals for α and β electrons this methodology partly takes into account the static correlation and is able to provide a good approximation of the charge density, even though it can potentially result in spin contamination and should not be used for the calculation of spin-density related properties.³⁵ To also capture long-range charge transfer contributions we use the cam-B3LYP functional with the 6-31G** basis set. A dispersion correction (Grimme's D3) is included to account for inter-molecular van der Waals interaction. This results in a meaningful computational approach to study the system at hand as discussed in more detail in our previous work, including a comparison of different computational schemes also with available experimental data.²⁵ We would like to note that energy differences between occupied and unoccupied molecular orbitals are known to be largely overestimated with the use of the cam-B3LYP functional for the materials studied here. Absolute band gap energies do

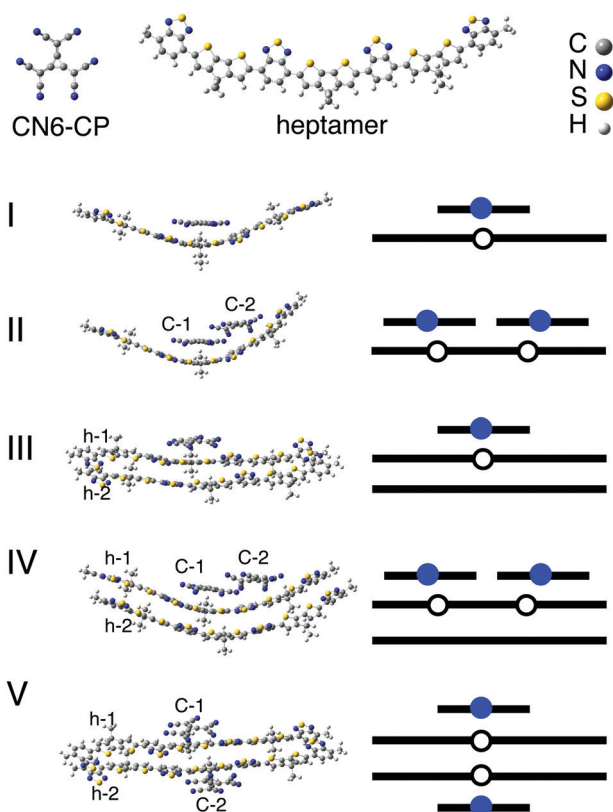


Fig. 1 Chemical structures of dopant molecule CN6-CP and PCPDT-BT heptamer. Integer charge transfer in the electronic ground state is found in complexes I–V, leading to different types of ICTC formation as schematically illustrated on the right. Dopant (heptamer) molecules in the complexes are labelled as C-1 and C-2 (h-1 and h-2). Short (long) bars represent the dopant molecule (PCPDT-BT heptamer) and filled (open) circles denote an excess electron (hole).

not compare well with corresponding experimental values^{25,29} such that only relative alignment and changes of energy levels for different systems should be interpreted as being physically relevant. In a first step the geometry of complex I was optimized and then used as a starting geometry to build complexes II to V by adding CN6-CP molecules and/or a conjugated chain. The geometries of complexes II–V were subsequently also optimized. All DFT calculations were performed with the GAUSSIAN09 package.³⁶ Hirshfeld charge partitioning was used to analyse the charge transfer between molecules, which for the systems studied leads to similar results as other charge partitioning scheme as detailed in our previous work.²⁵ The Hirshfeld charge partitioning and projected density of states were calculated using Multiwfn.³⁷

The heptamer:CN6-CP complexes studied are shown in Fig. 1, along with schematic illustrations of the ICTC formed in the electronic ground state of each complex. (for A-4)The dopant CN6-CP is considered a strong p-type dopant, for example studied in the doping of a diketopyrrolopyrrole (DPP)-based polymer for which efficient ICT formation was observed leading to greatly enhanced conductivity.³⁹ Our previous work also shows that the occurrence of ICT between PCPDT-BT and CN6-CP is quite robust and not sensitive to

the geometric details of the molecular complex.²⁵ In the present work we go beyond the bi-molecular PCPDT-BT:CN6-CP complex and report on ICT formation in complexes containing up to 2 polymer chains and 2 dopant molecules. The PCPDT-BT conjugated chains in the present study are represented by heptamers containing 3 PCPDT units and 4 BT units, which is significantly longer than the typical polaron expansion (less than 2 PCPDT units and 2 BT units) we find in this material,²⁵ such that the results are not much influenced by the quantum confinement in the finite-length conjugated chains.

With just one conjugated chain and one dopant molecule, complex I hosts a typical ICT scenario with charge transfer between the CN6-CP and the heptamer chain larger than $0.8 e$ (Table 1). A net charge transfer this large is already strongly indicative of the formation of an ICTC.²⁵ Besides a significant transfer of net charge, the occurrence of ICT in contrast to mere orbital hybridization is unambiguously evidenced in the spin-symmetry breaking found in the electronic ground state of complex I as discussed in detail below. Starting from complex I we now investigate the effect of increasing the number of dopant or conjugated molecules on the charge transfer observed. Our calculations show that with the addition of one CN6-CP molecule as in complex II a net positive charge of $1.68 e$ is induced on the conjugated chain. Accordingly the two CN6-CP molecules in complex II each carry a negative charge of about $0.84 e$. Therefore in the case of complex II double p-type doping of the PCPDT-BT heptamer occurs, induced by two nearby dopant molecules. In complex III, starting from complex I an additional PCPDT-BT heptamer is added to the complex. In this case a very similar overall electronic structure is found compared to complex I. To form complexes IV and V, respectively, both a CN6-CP molecule and a PCPDT-BT heptamer are added to complex I, with geometric arrangement of molecules qualitatively different in complexes IV and V though. In complex IV one heptamer is adjacent to both dopant molecules such that double doping is induced similarly to complex II but with qualitative differences in the electronic structure as discussed in detail below. In complex V each heptamer is singly doped with $0.84 e$ and $0.92 e$ net positive charge residing on the conjugated chains. For all complexes studied the net charges on each dopant and conjugated molecule are summarised in Table 1.

As visible in Fig. 1, the backbones of the heptamers can assume a somewhat bent (in complexes I, II, IV) or more planar geometry (in complexes III and V). This can be attributed to the complex interplay of the van der Waals interaction (computationally included through the dispersion correction) and

Coulomb interaction in the geometric optimization, which generally leads to quite closely packed molecular complexes and reshapes the heptamer's backbones as needed for energy minimization.³⁸ As we discussed earlier,²⁵ the backbone bending or torsion obtained after geometry optimization typically raises the HOMO energy on the order of $0.3 eV$, which may contribute but by itself is not sufficient to drive the ICT. Instead, the bending or torsion of the conjugated chain is partly the consequence of the charge transfer and related polaron formation. We note that in the optimized geometries of complexes III, IV and V, the π -stacked heptamers have similar interlayer spacing of around 3.7 \AA , which is close to typical GIWAXS data reported for similar systems.¹²

Complexes II and IV each contain a doubly doped heptamer, and complex V can be seen as two interacting ICTCs of the type of complex I. These three complexes possess unoccupied in-gap states on the doped heptamers that lie significantly lower in energy compared to their counterparts in complexes I and III. This can be seen in the calculated density of states projected onto each molecule which is shown in Fig. 2 for all five complexes studied. Comparing the energy positions of the unoccupied in-gap states on the oligomers in the different complexes is of particular interest here. These states are the doping-induced missing charge carriers or holes that once released to the OSC matrix lead to the formation of mobile charge carriers. The dashed lines in Fig. 2 at $-3.68 eV$ mark the center between an individual charge-neutral heptamer's HOMO and LUMO states as a reference. Also the calculated energy positions of a positive polaron on an individual PCPDT-BT heptamer and of the negative polaron on an individual CN6-CP molecule are included for comparison for the same geometries as assumed by these entities in complex I.

The calculated energies of the unoccupied in-gap states give a measure for the ICTC's tendency to release these holes to the surrounding OSC matrix. The results show that the in-gap states of complexes II, IV, V are significantly lower in energy than those of complexes I and III, such that a smaller activation energy would be needed to release a hole. It is also interesting to notice that for the doped heptamer h-1 in complex IV spin symmetry is almost recovered whereas all other complexes show significant spin asymmetry.

The reduced energy of in-gap states in complexes II, IV and V can be understood through the enhanced transfer of charges in these complexes, which modified the Coulomb potential. Taking complex V as an example, with the close proximity and repulsion of the two positively charged heptamers, for each heptamer the energy of the in-gap state is reduced. The doubly-doped heptamers in complexes II and IV can be interpreted as more extreme cases of two nearby doped heptamers as in complex V. It is worthwhile to have a closer look at the in-gap states of complexes II, IV, and V. For complex II, visualisation of these two (α and β) states in Fig. 3 shows a more localised and spatially separated charge distribution as a pair of so-called side-by-side polarons is formed.⁴⁰ The in-gap states of complex IV have a significantly different spatial distribution. The α and β orbitals are spatially not separated but overlapping with each other, and are delocalised over almost the entire length of the

Table 1 Hirshfeld charges on the conjugated chains and CN6-CP molecules in complexes I–V. C-1 and C-2 refer to the CN6-CP molecules, and h-1 and h-2 refer to the conjugated chains according to the labels in Fig. 1

	C-1	C-2	h-1	h-2
I	$-0.86 e$	—	$0.86 e$	—
II	$-0.83 e$	$-0.85 e$	$1.68 e$	—
III	$-0.91 e$	—	$0.87 e$	$0.04 e$
IV	$-0.83 e$	$-0.88 e$	$1.64 e$	$0.07 e$
V	$-0.86 e$	$-0.90 e$	$0.84 e$	$0.92 e$

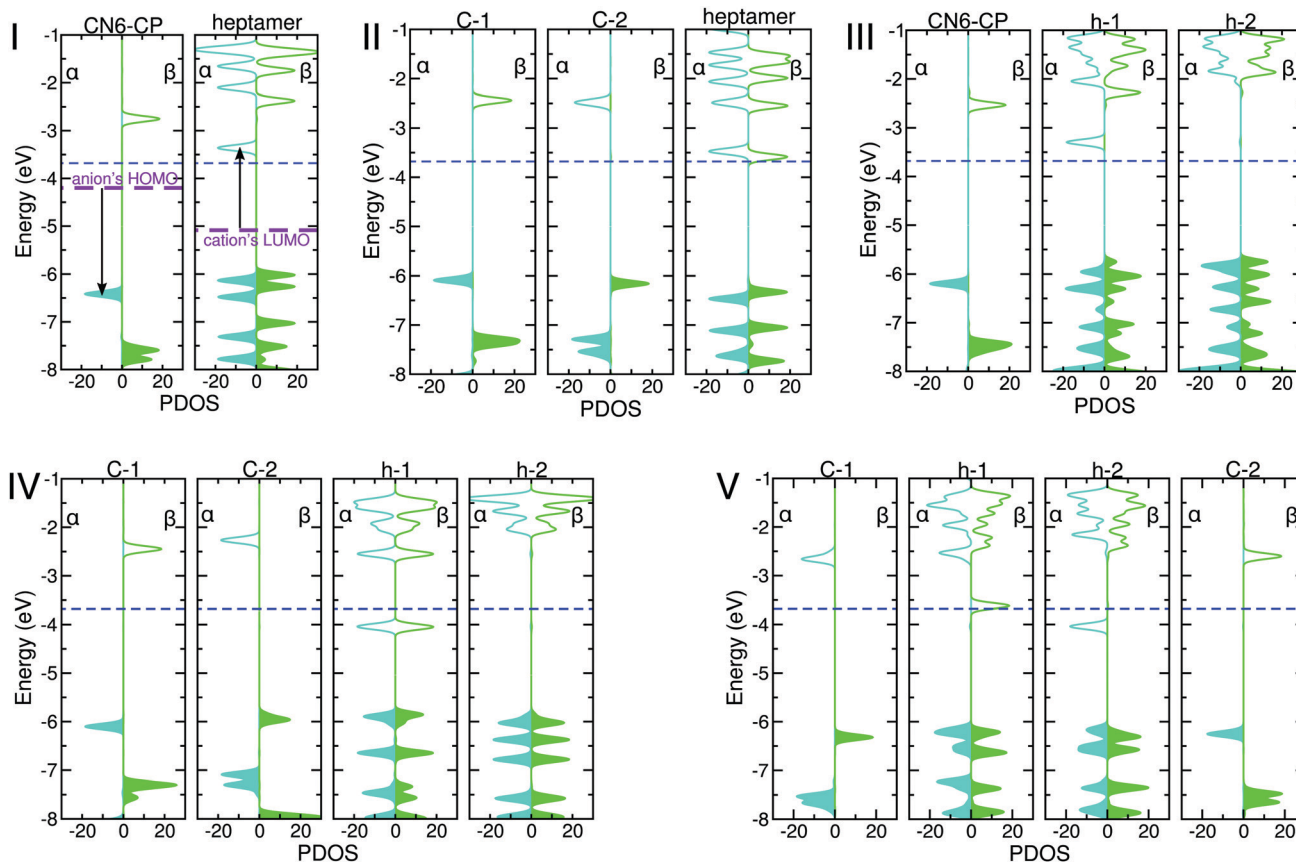


Fig. 2 Calculated projected density of states (PDOS) for α and β spin channels for each molecule in complexes I–V in Fig. 1. For each sub-panel α and β components are shown as positive and negative values on the horizontal axis, respectively. C-1, C-2, h-1, and h-2 label the PDOS of the corresponding molecules in each complex as introduced in Fig. 1. Shaded areas mark occupied electronic states. The blue dashed line at -3.68 eV marks the center between an individual neutral heptamer's calculated HOMO and LUMO energies. Panel I: for comparison the purple lines in the first panel mark the calculated HOMO (LUMO) of a positive (negative) polaron on an individual isolated PCPDT-BT heptamer (CN6-CP molecule) in the same geometry as assumed by the heptamer (CN6-CP) in complex I. The arrows indicate the energy shift of the levels upon forming the ICTC. We note that energy differences between occupied and unoccupied states (or in other words band-gap energies) are largely overestimated with the cam-B3LYP DFT functional used, only relative energy level alignment and changes of energy levels for different systems are physically meaningful.

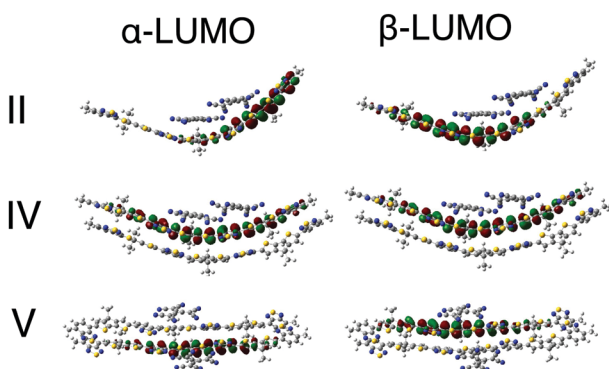


Fig. 3 Isosurfaces of LUMO orbitals of complexes II, IV and V. These represent the two doping-induced positive charges on the conjugated chains in the complexes depicted.

oligomer as shown in Fig. 3. In this case a bi-polaron state is formed.⁴⁰ The lower energy and more pronounced delocalisation of the in-gap states of complex IV with respect to those of complex II illustrate the role of the additional h-2 heptamer in

the complex. For a closer analysis we also performed calculations for a complex with two stacking heptamers as in complex IV or V (and no dopant molecules) with $2e$ positive net charge, namely a polaron dimer. However, in these calculations formation of a pair of side-by-side polarons on one of the two chains was found, similar to the side-by-side polarons in complex II. So the observations in complex IV can neither only be attributed to the presence of the two CN6-CP dopant molecules nor to the presence of two PCPDT-BT heptamers but more so to their combined effect on the electronic states. The α and β in-gap states of complex V are positioned on different conjugated chains in the complex such that more of the original behavior of the singly doped complex I is preserved, resulting in an in-gap state energetics that is somewhere in between those of complex I and complex IV. Interestingly, these results also shed some light on the behavior of two interacting polarons on PCPDT-BT chains in different molecular environments. We find that those form a side-by-side polaron in an isolated polaron dimer as in complex II, a bi-polaron in complex IV, and remain as two individual polarons on different

chains in complex V. It is important to mention that the doubly-doped PCPDT-BT in complex II can not be understood from a single-electron picture, since neither the HOMO of the PCPDT-BT:CN6-CP pair or of complex I (-6.01 eV by cam-B3LYP), nor the HOMO of a PCPDT-BT polaron (-7.47 eV by cam-B3LYP) can explain the second ICT to the LUMO of the CN6-CP (-5.03 eV by cam-B3LYP). Instead, we find that the double ICT in complex II and IV has to be interpreted as a collective effect in the complex containing three or more molecules.⁴² The spatial expansion has been an important aspect in the studies of side-by-side polarons. The experimental data about side-by-side polarons typically indicate an expansion of several nm for one polaron with significant separation in between.^{40,43} The side-by-side polarons found in the present work show a shorter length, covering almost the whole backbone of the heptamer (around 4 nm in length) without any actual separation or even penetrating into each other (e.g. Fig. 3 II), which could be either system-dependent or a result of the finite-length conjugated chain.

As mentioned above, the choice of CN6-CP as dopant in the present study is partly motivated by the robust observation of ICT, whereas other widely studied dopants such as F4TCNQ or F6TCNNQ have been found to show either ICT formation or orbital hybridization depending on geometrical details.^{25,39} In the present work we find that even for CN6-CP the systematic observation of the two-fold ICT requires reasonably compact and stacked molecule/polymer complexes. This implies that the experimental observation of isolated such larger ICTC complexes in solution rather than molecular films may be challenging.⁴¹

It was recently suggested that the electron-hole Coulomb binding energy in ICTCs plays a crucial role in determining the thermal activation energy of molecularly doped organic semiconductors.²³ In the present work the ICTCs of different sizes and with different amounts of transferred charge provide an ideal platform to directly analyze the Coulomb binding energies based on a molecular level and the microscopic DFT approach. To this end we performed BS-DFT calculations for ICT complexes I–V with an $1 e$ additional negative charge. This reduces the net charge on conjugated chains to almost zero positive net charge for the originally singly doped heptamer, and to close to $1 e$ positive net charge on the heptamers originally experiencing double doping. As illustrated in Fig. 4, the Coulomb binding energies for each complex are then estimated as the difference between (i) the sum of the total energies of a neutral ICTC and a neutral heptamer (representing the energetics before releasing the doping-induced positive charge to the OSC matrix), and (ii) the sum of total energies of the corresponding negatively charged ICTC and a singly positively charged heptamer (representing the energetics after release of the doping-induced positive charge into the OSC matrix). This definition is equivalent to the difference between the electron affinity (EA) of an ICTC and the ionisation energy (IE) of a single conjugated chain, which was used in ref. 23. To remove the effect of geometric change upon changing the charge configuration, the geometries of the ICTCs were fixed to the ones of the respective overall neutral structures. The results show that the calculated Coulomb binding energies

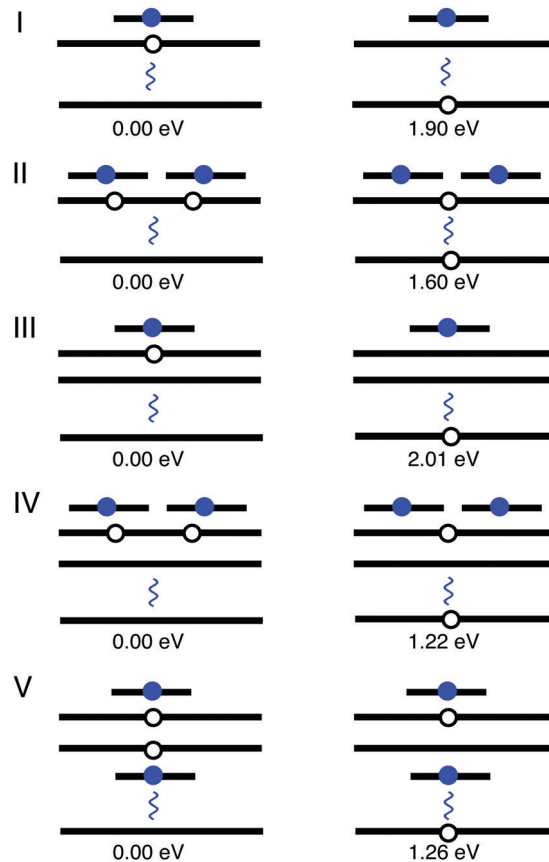


Fig. 4 Schematic of the ICTCs before and after charge release to a PCPDT-BT matrix as discussed in the text. For each panel, on the left (right) the system is shown before (after) charge release. The wavy lines indicate the assumption of full release of the doping-induced positive charge to the surrounding PCPDT-BT matrix such that the distance of the released charge to the original ICTC is assumed to be infinite. Energies needed to release the charge are given for each complex on the right. The reference energies 0.0 eV are set for each complex separately as described in the text.

needed to be overcome for the release of one hole are significantly reduced in the doubly doped complexes II, IV and V (with 1.60 eV, 1.22 eV, 1.26 eV) compared to those of complexes I and III (with 1.90 eV and 2.01 eV). This can also be equivalently interpreted as the increased EAs of complexes II, IV, V. We note that differences in these Coulomb binding energies from one ICT complex to another directly correlate with changes of the in-gap state energies in Fig. 2, but for the former also absolute values obtained are physically more meaningful as these Coulomb binding energies have directly been obtained from total energy considerations. The values obtained here are in the same range as those calculated for different systems in ref. 23.

The reduced Coulomb binding energies of the doping-induced charges in complexes IV and V are particularly noticeable. In a simplified picture these can be attributed to electrostatic interactions brought about by the close proximity of effectively two ICT complexes as parts of one bigger complex. After accepting an electron or effectively releasing a hole,

complex IV and V each still consist of two anionic CN6-CPs and one cationic PCPDT-BT chain. The Coulomb interactions between these charged molecules effectively leads to an additional stabilisation and increased EA compared to the case of one single anionic CN6-CP that remains after charge release in complexes I and III.

The different ICTCs with released charges are illustrated in Fig. 4 in the panels on the right. The effect of reduced Coulomb binding of the doping-induced charges is less pronounced in complex II which is rooted in the charge density that is only confined to a single heptamer. We would like to point out that the complexes explicitly studied in the present work illustrate the basic electronic mechanisms that occur in ICTC consisting of more than one doped conjugated chain and counterion. In a molecular film environment various geometrical configurations are expected to contribute to the overall energetics of the electronic landscape, potentially also including clusters of dopant or conjugated molecules and areas with reduced order and crystallinity caused by inclusion of the dopant such that all the scenarios discussed above are eventually expected to contribute to charge carrier densities and the final conductivity in p-doped OSCs. Also, in the present work only the first step beyond a single pair of dopant molecule and conjugated chain is taken. The addition of further ICTCs and conjugated chains is expected to further reduce the Coulomb binding of doping-induced charges for certain larger ICTC configurations, to an extent that would also depend on structural details.

We would further like to discuss that the hypothesised charge release process illustrated in Fig. 4 contains the CN6-CP and conjugated chain molecules but still assumes releasing the hole to the OSC matrix represented by a neutral conjugated chain. This scenario should be applicable to an intermediate doping density and is different from the high doping limit discussed by Leo *et al.*,²³ where the charge transport takes place between ICTCs. Furthermore, since the increased EA values of complex IV and V originate from the multi-molecule interactions inside the complexes, they have a different nature from the recently discussed broadened EA distribution, or energetic disorder, mainly caused by diversified local environments of individual ICTCs, although both can contribute to the reduced Coulomb binding energy.

3 Conclusions

In the present work we investigated the molecular p-type doping of organic semiconductor materials by DFT calculations and obtain insights on a molecular level. Specifically, we studied in detail the electronic structure of PCPDT-BT:CN6-CP ICTCs of different sizes. An important finding is that the formation of multi-molecule ICTCs with enhanced CT behaviour can significantly reduce the energy cost of releasing the doping-induced charges to the host matrix. In systems larger than just a single bi-molecular ICTC, the increased number of conjugated chains and dopant molecules allows for different electronic processes to contribute, including doubly-doped conjugated chains or

interacting adjacent singly-doped conjugated chains. Those ICTCs containing two bi-molecular ICTCs show significantly increased EA, and therefore reduced Coulomb binding energy for the doping-induced positive charges on the conjugated chains (holes) compared to that in individual bi-molecular ICTC. In a simplified picture this can be explained by electrostatic interactions inside the complexes and is reflected in our detailed calculations of the electronic structure. Overall, our results provide valuable insight into the interplay of different electronic processes important for efficient molecular doping of OSC films, including interaction of adjacent bi-molecular ICTCs.

Conflicts of interest

There are no conflicts to declare.

Acknowledgements

We acknowledge funding from the Deutsche Forschungsgemeinschaft through project SCHU 1980/13 and through the Heisenberg program (No. 270619725). A grant for computing time at the Paderborn Center for Parallel Computing (PC²) is gratefully acknowledged.

Notes and references

- 1 S. Reineke, F. Lindner, G. Schwartz, N. Seidler, K. Walzer, B. Lüssem and K. Leo, *Nature*, 2009, **459**, 234–238.
- 2 B. Lüssem, M. L. Tietze, H. Kleemann, C. Hoßbach, J. W. Bartha, A. Zakhidov and K. Leo, *Nat. Commun.*, 2013, **4**, 2775.
- 3 K. H. Yim, G. L. Whiting, C. E. Murphy, J. J. M. Halls, J. H. Burroughes, R. H. Friend and J. S. Kim, *Adv. Mater.*, 2008, **20**, 3319–3324.
- 4 D. T. Duong, C. Wang, E. Antono, M. F. Toney and A. Salleo, *Org. Electron.*, 2013, **14**, 1330–1336.
- 5 B. Lüssem, M. Riede and K. Leo, *Phys. Status Solidi A*, 2013, **210**, 9–43.
- 6 I. E. Jacobs and A. J. Moulé, *Adv. Mater.*, 2017, **29**, 1703063.
- 7 P. Pingel and D. Neher, *Phys. Rev. B: Condens. Matter Mater. Phys.*, 2013, **87**, 115209.
- 8 E. E. Aziz, A. Vollmer, S. Eisebitt, W. Eberhardt, P. Pingel, D. Neher and N. Koch, *Adv. Mater.*, 2007, **19**, 3257–3260.
- 9 P. Beyer, D. Pham, C. Peter, N. Koch, E. Meister, W. Brütting, L. Grubert, S. Hecht, D. Nabok, C. Cocchi, C. Draxl and A. Opitz, *Chem. Mater.*, 2019, **31**, 1237–1249.
- 10 I. Salzmann, G. Heimel, M. Oehzelt, S. Winkler and N. Koch, *Acc. Chem. Res.*, 2016, **49**, 370–378.
- 11 B. Neelamraju, K. E. Watts, J. E. Pemberton and E. L. Ratcliff, *J. Phys. Chem. Lett.*, 2018, **9**, 6871–6877.
- 12 H. Méndez, G. Heimel, S. Winkler, J. Frisch, A. Opitz, K. Sauer, B. Wegner, M. Oehzelt, C. Röthel, S. Duhm, D. Többsen, N. Koch and I. Salzmann, *Nat. Commun.*, 2015, **6**, 8560.
- 13 K. E. Watts, B. Neelamraju, E. L. Ratcliff and J. E. Pemberton, *Chem. Mater.*, 2019, **31**, 6986–6994.
- 14 D. Kiefer, *et al.*, *Nat. Mater.*, 2019, **18**, 149–155.

- 15 M. L. Tietze, J. Benduhn, P. Pahner, B. Nell, M. Schwarze, H. Kleemann, M. Krammer, K. Zojer, K. Vandewal and K. Leo, *Nat. Commun.*, 2018, **9**, 1182.
- 16 F. Ghani, A. Opitz, P. Pingel, G. Heimel, I. Salzmann, J. Frisch, D. Neher, A. Tsami, U. Scherf and N. Koch, *J. Polym. Sci., Part B: Polym. Phys.*, 2015, **53**, 58–63.
- 17 P. Pingel, L. Y. Zhu, K. S. Park, J. O. Vogel, S. Janietz, E. G. Kim, J. P. Rabe, J. L. Bredas and N. Koch, *J. Phys. Chem. Lett.*, 2010, **1**, 2037–2041.
- 18 J. H. Lee, J. Lee, Y. H. Kim, C. Yun, B. Lüssem and K. Leo, *Org. Electron.*, 2014, **15**, 16–21.
- 19 P. K. Koech, A. B. Padmaperuma, L. A. Wang, J. S. Swensen, E. Polikarpov, J. T. Darsell, J. E. Rainbolt and D. J. Gaspar, *Chem. Mater.*, 2010, **22**, 3926–3932.
- 20 D. Di Nuzzo, C. Fontanesi, R. Jones, S. Allard, I. Dumsch, U. Scherf, E. von Hauff, S. Schumacher and E. Da Como, *Nat. Commun.*, 2015, **6**, 6460.
- 21 M. Zamadar, S. Asaoka, D. C. Grills and J. R. Miller, *Nat. Commun.*, 2013, **4**, 2818.
- 22 A. Mityashin, Y. Olivier, T. Van Regemorter, C. Rolin, S. Verlaak, N. G. Martinelli, D. Beljonne, J. Cornil, J. Genoe and P. Heremans, *Adv. Mater.*, 2012, **24**, 1535–1539.
- 23 M. Schwarze, *et al.*, *Nat. Mater.*, 2019, **18**, 242–248.
- 24 V. Arkhipov, E. Emelianova, P. Heremans and H. Bässler, *Phys. Rev. B: Condens. Matter Mater. Phys.*, 2005, **72**, 235202.
- 25 C. Dong and S. Schumacher, *J. Phys. Chem. C*, 2019, **123**, 30863–30870.
- 26 L. Zhu, E. Kim, Y. Yi and J. L. Brédas, *Chem. Mater.*, 2011, **23**, 5149–5159.
- 27 A. M. Valencia and C. Cocchi, *J. Phys. Chem. C*, 2019, **123**, 9617–9623.
- 28 K. A. Thomas, D. B. Datko and J. K. Grey, *J. Phys. Chem. C*, 2020, **124**, 2137–2145.
- 29 Y. Karpov, *et al.*, *Macromolecules*, 2017, **50**, 914–926.
- 30 C. Wiebeler, R. Tautz, J. Feldmann, E. von Hauff, E. Da Como and S. Schumacher, *J. Phys. Chem. B*, 2013, **117**, 4454–4460.
- 31 R. Tautz, *et al.*, *J. Am. Chem. Soc.*, 2013, **135**, 4282–4290.
- 32 J. Gao, J. D. Roehling, Y. Li, H. Guo, A. J. Moulé and J. K. Grey, *J. Mater. Chem. C*, 2013, **1**, 5638–5646.
- 33 A. M. Valencia, M. Guerrini and C. Cocchi, *Phys. Chem. Chem. Phys.*, 2020, **22**, 3527–3538.
- 34 J. Li, G. D'Avino, A. Pershin, D. Jaquemin, I. Duchemin, D. Beljonne and X. Blase, *Phys. Rev. Mater.*, 2017, **1**, 025062.
- 35 F. Neese, *Coord. Chem. Rev.*, 2009, **253**, 526–563.
- 36 M. J. Frisch, *et al.*, *Gaussian 09, Revision D.01*, Gaussian, Inc., Wallingford, CT, 2009.
- 37 T. Lu and F. Chen, *J. Comput. Chem.*, 2012, **33**, 580–592.
- 38 C. Dong, H. Hoppe and W. Beenken, *J. Phys. Chem. A*, 2016, **120**, 3835–3841.
- 39 Y. Karpov, *et al.*, *Adv. Mater.*, 2016, **28**, 6003–6010.
- 40 L. Zaikowski, *et al.*, *J. Am. Chem. Soc.*, 2012, **134**, 10852.
- 41 I. E. Jacobs, *et al.*, *J. Mater. Chem. C*, 2016, **4**, 3454.
- 42 H. Huang, C. Karlsson, F. Mamedov, M. Strømme, A. Gogoll and M. Sjödin, *J. Phys. Chem. C*, 2017, **121**, 13078–13083.
- 43 J. Bakalis, A. R. Cook, S. Asaoka, M. Forster, U. Scherf and J. R. Miller, *J. Phys. Chem. C*, 2014, **118**, 114–125.